Applied Computer Science, vol. 20, no. 3, pp. 192–201
doi: 10.35784/acs-2024-36

Submitted: 2024-09-06 | Revised: 2024-09-26 | Accepted: 2024-09-29

Keywords: diesel engine, PI control, algorithm, speed regulation, helicopter propulsion

Paweł MAGRYTA [0000-0002-9654-2909]*, *Grzegorz BARAŃSKI* [0000-0003-2596-3148]*

SIMULATION OF TORQUE VARIATIONS IN A DIESEL ENGINE FOR LIGHT HELICOPTERS USING PI CONTROL ALGORITHMS

Abstract

This article presents the results of simulation research of a diesel engine for a light helicopter. The simulations were performed using the 1D software AVL Boost RT. The engine model includes elements such as cylinders, turbine, compressor, inlet and outlet valves, ambient environment definition, and fuel injection control strategy. The simulations aimed to evaluate the engine's response to step changes in the main rotor load, both increasing and decreasing power demands. Parameters analyzed included power deviation, torque, engine rotational speed, and stabilization time of the main rotor rotational speed. All tests were conducted using a single set of PI controller settings. The results demonstrate that these parameters are dependent on the magnitude of the step change in the main rotor load demand. The study compares the maximum engine rotational speed deviation from the nominal value for both increasing and decreasing main rotor load demands. The findings indicate that using PI regulator to control rotational speed in the diesel engine in a light helicopter significantly depends on the change in the load torque on the rotor.

1. INTRODUCTION

Recent advancements in aviation technology necessitate increasingly sophisticated control methods to ensure optimal performance and safety under various operating conditions (Hlinka et al., 2021). This requirement is particularly critical in the helicopter industry. In the case of helicopters, control of main rotor rotational speed is crucial for reasons of safety and fuel economy. During flight, the helicopter is subjected to varying aerodynamic conditions that change the pressure fields around the operating rotor. Consequently, this leads to changes in the moments and power required to drive the rotor. Rotational speed control of the main rotor, which involves forced torque variation, is crucial for maintaining flight stability and efficiency (Dudnika & Gaponova, 2022). Thus, it is reasonable to maintain a constant rotational speed of the helicopter power unit. The essence of this issue is topical, as indicated by ongoing scientific work (Wang et al., 2023a; Zang et al., 2013).

Different propulsion units require different approaches to how to control the power unit. The research presented in this article focuses on the propulsion unit of a light helicopter equipped with a diesel engine (Magryta & Majczak, 2012). The reason for trying to use a diesel engine in a light helicopter is to reduce fuel and toxic emissions compared to a turboshaft engine (Wendeker et al., 2014). However, in this case, precise modeling and control of the engine (main rotor) rotational speed are essential for optimizing helicopter performance (Pietrykowski et al., 2014). Similar considerations apply to other aerial devices such as gyrocopters (Czyż et al., 2016). Modeling the rotational speed of a diesel engine in a light helicopter context is complex, requiring the consideration of numerous factors, including the engine's mechanical and thermodynamic characteristics, the dynamics of fuel and air flows, and changing environmental conditions (Heywood, 1988; Stone, 1992). These factors impact the main flight parameters, passenger comfort, and environmental considerations (Łusiak & Grudzień, 2013). Although many diesel engine modeling approaches exist, they typically focus on land or marine applications, with relatively little attention to aircraft engines (Mueller, 2002).

* Lublin University of Technology, Faculty of Mechanical Engineering, Department of Thermodynamics, Fluid Mechanics and Aviation Propulsion Systems, Poland, p.magryta@pollub.pl, g.baranski@pollub.pl

The PID (Proportional-Integral-Derivative) algorithm is widely used in control systems for its simplicity and efficiency (Åström & Murray, 2008; Przystupa, 2018). It is an algorithm that does not require advanced tuning methods, but only the selection of appropriate parameter settings. In light helicopter diesel engine control, PID fine-tunes control parameters to maintain engine stability and performance under varying flight conditions (Ang et al., 2005). The algorithm efficiently responds to changes in engine load and operating conditions, which is essential in aerospace applications requiring rapid and precise control (Wang et al., 2023b). Widespread use of these algorithms is even found in unmanned aerial vehicles (UAV). For example (Czyż et al., 2023) used a PID controller for a PWM value control algorithm for a servomotor. Feedback control enables precise, repeatable load setting at nodes. It also protects against overloading the hull structure. Other algorithms are also used in the combustion engine industry, such as adaptive algorithms. They are able to respond to changes in a more dynamic way, however, their construction and operating principle are much more complicated (Banaszuk et al., 2004).

This article details the modeling process of torque variation effects on the rotational speed of a light helicopter diesel engine and the application of the PI algorithm for its control (Omran et al., 2024). The implementation of the PI algorithm in the engine model is presented, and computer simulations evaluate the effectiveness of this approach under different torque variation scenarios.

2. MODEL DESCRIPTION

A diesel engine model for a light helicopter was created using AVL Boost RT software (Beller et al., 2021). The model includes an internal combustion engine, a helicopter gear element, and a rotor. The engine is a V8 design with a 4400 cm3 capacity and 330 kW maximum power. The engine was designed to be used in the new kind of light helicopter that was the subject of the DELILAH (Diesel Engine Matching The Deal Light Platform ff The Helicopter) project made under Clean Sky consortium. The view of the model is presented in Fig. 1. The model consists of several components. At the top of the model, you can see the compressor (Compressor 1), which draws air from the environment (Ambient 1) and pumps it through pipes into the cylinder (Cylinder 1) of the engine (Engine 1). The model also takes into account the exchange of heat with the environment (Heat Transfer), which affects the efficiency of the system's operation. On the left side of the diagram is the turbine (Turbine 1), which also discharges air into the environment (Ambient 2) and supplies energy to the shaft (Shaft 1). The fuel system consists of a fuel tank (Fuel Tank 1), and the fuel flow control (Mass Flow 1). An important part of the model is the section (Speed Control), responsible for regulating engine rotational speed. It uses a PI controller to control the fuel supply (Fuelling) and to monitor the difference between the target speed (TargetSpeedDiff) and the actual speed. Elements of this subsystem include control functions and PI controllers that take care of maintaining a stable rotational speed. At the output, the engine drives a shaft (Shaft 2), which in turn transmits power to a transmission system (Single Ratio Transmission) and ultimately to a mechanical consumer (Mechanical Consumer 1), which represents a helicopter rotor. This model allows the simulation of the dynamics of the diesel engine under real operational conditions of the helicopter, taking into account variable parameters such as fuel supplied, speed, and airflow.

The operational condition for the diesel engine is to maintain a constant rotational speed of 3500 rpm, dictated by the helicopter's design and power requirements. A detailed description of the model is presented in the publication (Magryta, 2021).

Simulation tests evaluated the engine's response to load spikes of rotor torque during helicopter flight. Spikes in helicopter rotor load demand corresponding to sudden changes in pressure fields around the rotor were chosen. They can represent variable situations occurring during helicopter flight resulting from helicopter maneuvers, sudden gust elevators or approaching obstacles. Load changes involved stepwise torque variations on the main rotor, corresponding to power spikes (1, 2, 3, 5, 10, 20, 30, 40, and 50 kW) from 80 to 130 kW (increasing) and from 130kW to 80kW (decreasing). The selected range of torque changes represents one of many among the tests conducted. Such a range of changes was chosen as representative because authors plan, in the future, to compare the simulation tests performed with real tests on a dynamometer equipped with an engine of less than the assumed 330 kW power. Therefore, the studies presented in the article are for the range of reduced engine power.

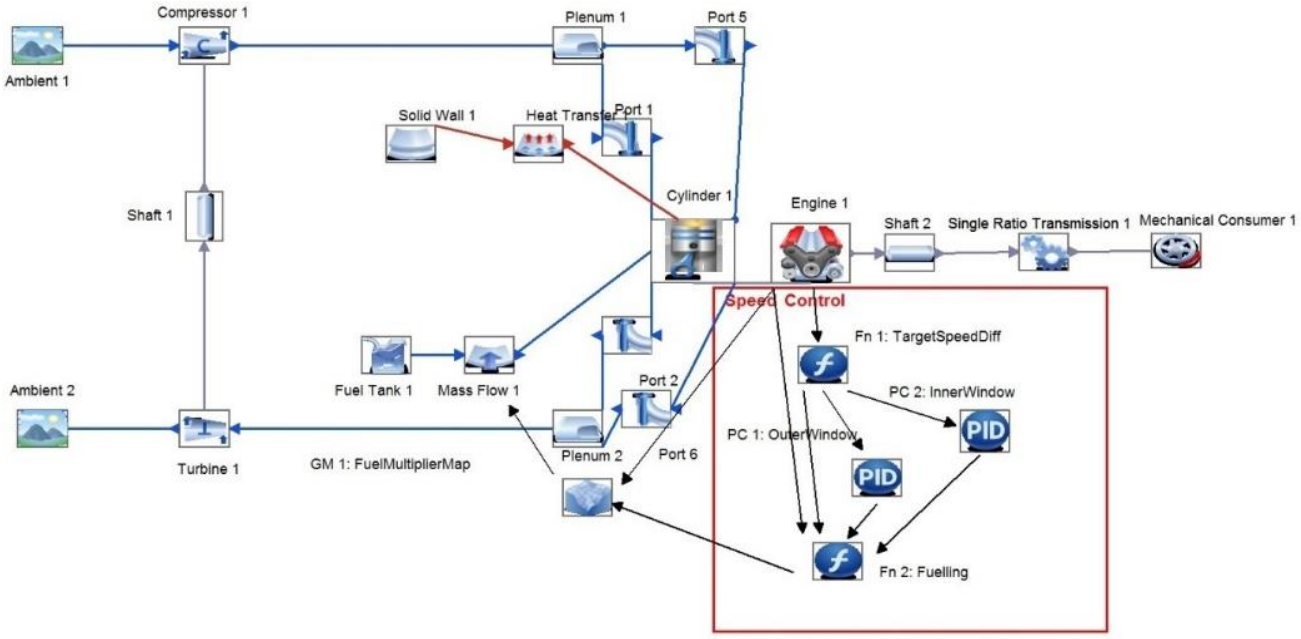

Fig. 1. Diesel engine model made in AVL Boost RT software (Magryta, 2021)

These variations were tested in both increasing and decreasing power demand scenarios. Parameters such as power, torque, and main rotor rotational speed were recorded. All tests were made using a single PI controller setting. The changes were implemented according to the table below, which includes 18 research points, each representing a distinct scenario. The scenarios for increasing engine power are numbered from 1 to 9 (Tab. 1), while those for decreasing power are numbered from 11 to 19 (Tab. 2). The number 10 was omitted to facilitate easier comparison of corresponding points between the two sets.

Tab. 1. Power and torque values for power increase scenarios

Scenario no.	1.	2.	3.	4.	5.	6.	7.	8.	9.
Starting engine power [kW]	80	80	80	80	80	80	80	80	80
Finishing engine power [kW]	81	82	83	85	90	100	110	120	130
Power change [kW]	1	2	3	5	10	20	30	40	50
Starting engine torque [Nm]	218.27	218.27	218.27	218.27	218.27	218.27	218.27	218.27	218.27
Finishing engine torque [Nm]	221.00	223.73	226.45	231.91	245.55	272.84	300.12	327.40	354.69

Tab. 2. Power and torque values for power decrease scenarios

Scenario no.	11.	12.	13.	14.	15.	16.	17.	18.	19.
Starting engine power [kW]	130	130	130	130	130	130	130	130	130
Finishing engine power [kW]	129	128	127	125	120	110	100	90	80
Power change [kW]	-1	-2	-3	-5	-10	-20	-30	-40	-50
Starting engine torque [Nm]	354.69	354.69	354.69	354.69	354.69	354.69	354.69	354.69	354.69
Finishing engine torque [Nm]	351.96	349.23	346.50	341.05	327.40	300.12	272.84	245.55	218.27

In an earlier study conducted using the same model (Magryta, 2021), the authors analyzed the change in P setting on the time course of engine rotational speed. As in the current study, the D setting was 0, and the I

setting varied slightly. The results from earlier studies showed that the P setting in the range from -0.0003 to -0.0004 gives the smallest control error. Earlier studies also shown that changing the D parameter value for different than 0 results in longer stabilization of rotational speed signal. Taking the above into account, it was decided to conduct tests using the following PI controller setting with the following parameters: P = -0.00035, I = -0.002 and D = 0.

The rotational speed control of the Diesel engine was done by changing the fuel injection timing (output value). The control setpoint was to maintain a constant rotational speed of 3500 rpm. The value that disturbed the operation of the system was defined as torque spikes. The control scheme is shown in Fig. 2 (Niederliński et al., 1995).

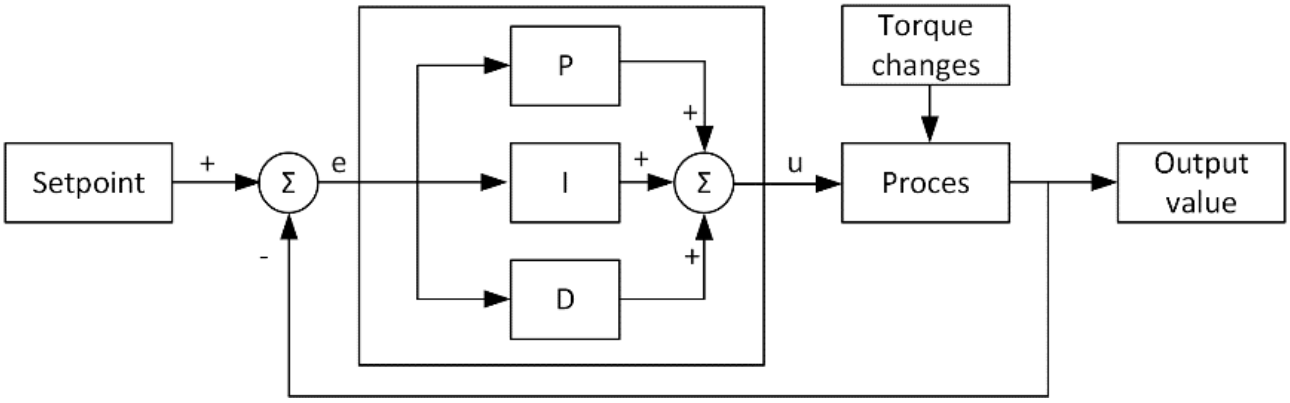

Fig. 2. Diagram of diesel engine speed control in a helicopter

The output value of the PI controller, or control signal u(t), is expressed by the formula:

$$u(t) = P \cdot e(t) + I \cdot \int_0^t e(t)dt + D \cdot \frac{de(t)}{dt} \tag{1}$$

where: *e(t)* – regulation error,
P – proportional gain,
I – integral gain,
D – differential gain,
T – time.

The total simulation time was 12 seconds. Power and torque changes were introduced in the 7th second, as the model required approximately 5 seconds to stabilize after each startup. Stabilization was determined by the absence of significant changes in the set rotational speed value (lower than 1 rpm) for the next 5 consecutive time steps. The total simulation time step was 17.5 ms for each research point.

3. RESULTS AND DISCUSSION

To visualize the results, the first 6 seconds of the simulation (stabilization time from startup) were omitted from the graphs. The results show the engine rotational speed curve's response to different scenarios, with distinct graphs for increasing and decreasing power. The graphs illustrate the engine rotational speed curves under various scenarios. Figure 3 depicts cases of increasing power, while Fig. 4 shows cases of decreasing power. As can be seen in the figures, the rotational speed changes significantly when torque spikes occur. For an increase in power demand, the engine speed decreases, while for a decrease in power demand, the situation is reversed. The maximum values of speed deviation are highest when the change in engine power and torque demand is greatest (scenario 9 and scenario 19). They reach the difference of 13 and 14 rpm.

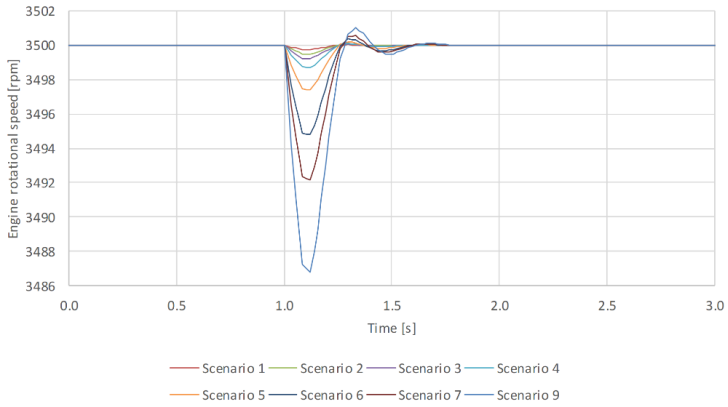

Fig. 3. The time course of the engine rotational speed for different scenarios, for increasing power

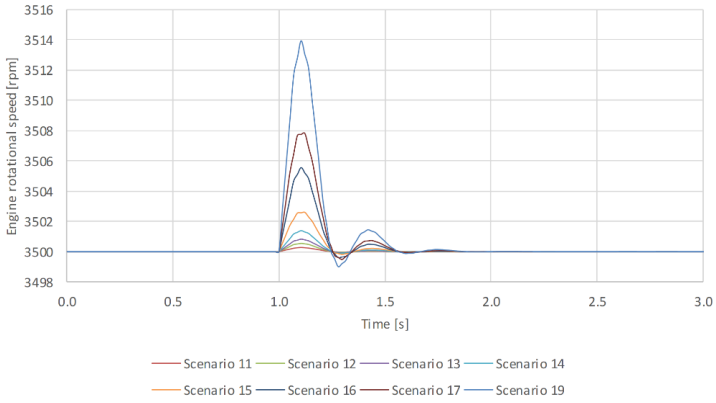

Fig. 4. The time course of the rotational engine speed for different scenarios, for decreasing power

The next results show the characteristics of:

- total rotational speed differences n_t [rpm·s],
- rotational speed differences n_{dif} [%],
- stabilization time S_t [%].

Those parameters are calculated separately for scenario 1-9 (increasing power) and scenario 11-19 (decreasing power). The significance of all parameters is presented graphically in Fig. 5.

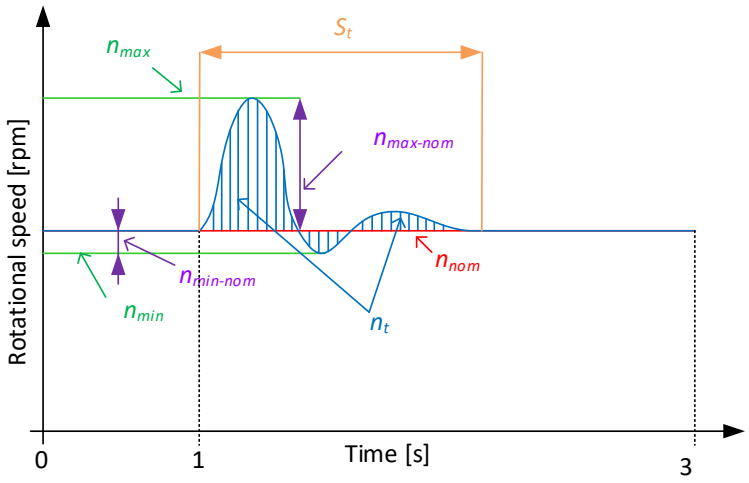

Fig. 5. Graphical visualization of calculation parameters

The parameter of total rotational speed differences nt was calculated by integrating the rotational speed curve against the nominal speed value. As presented in Fig. 6-7 the parameter nt maintains a linear relationship

as a function of both increasing engine power and decreasing engine power. It should be noted that for the maximum value of engine power variation, i.e. 50 kW, the parameter shows a higher value, i.e. 2.22 rpm·s for increasing power (scenario 9) compared to 2.17 rpm·s for decreasing power (scenario 19).

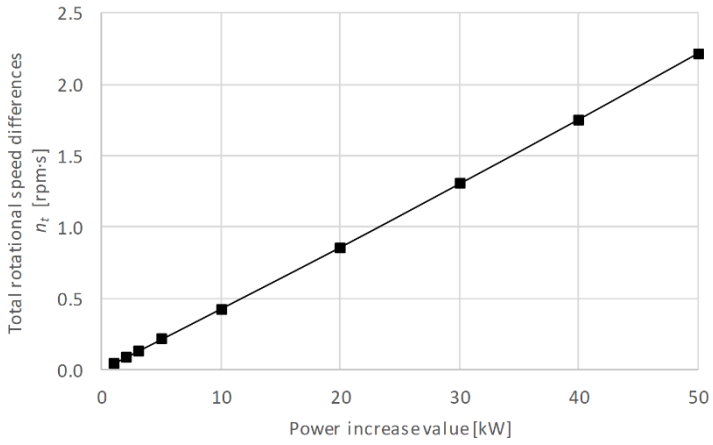

Fig. 6. Total rotational speed differences n_t for scenarios 1-9 (power increase)

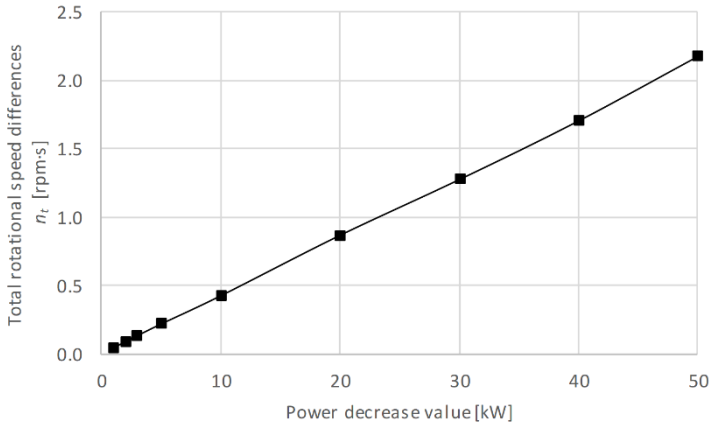

Fig. 7. Total rotational speed differences n_t for scenarios 11-19 (power decrease)

The parameter of rotational speed differences n_{dif}, was calculated as the largest value from $n_{min\text{-}nom}$ or $n_{max\text{-}nom}$ related by percentage to the n_{nom} value, according to the equation below. A value of 3500 rpm was taken as n_{nom}.

$$n_{dif} = \frac{n_{min-nom} \vee n_{max-nom}}{n_{nom}} \cdot 100\% \quad (2)$$

where: $n_{min-nom}$ – largest value between minimal and nominal rotational speed,
$n_{max-nom}$ – largest value between maximal and nominal rotational speed,
n_{nom} – nominal rotational speed.

The next two Fig. 8-9 show the dependence of the rotational speed differences parameter n_{dif} on increasing engine power as well as decreasing engine power. As can be seen from the accompanying figures, both values show a linear relationship. However, in this case, the maximum value for a power change of 50 kW is higher for decreasing power and is 0.00398% (scenario 19) compared to the identical point for increasing power of 0.00377% (scenario 9).

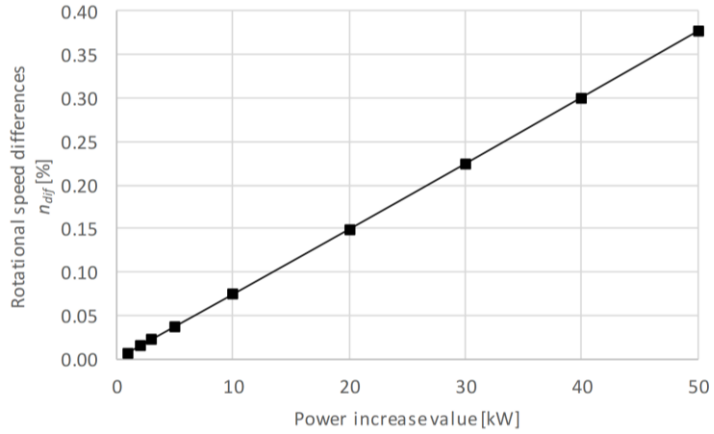

Fig. 8. Rotational speed differences n_{dif} for scenario 1-9 (power increase)

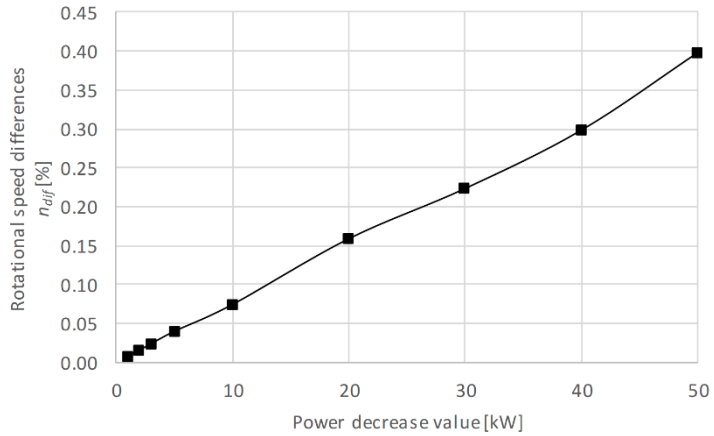

Fig. 9. Rotational speed differences n_{dif} for scenario 11-19 (power decrease)

Similarly, the values of power and torque deviation behave in a linear manner, which is not shown graphically, since they are related by a constant mathematical relationship to the previously presented parameters. The next Fig. 10-11 show the values of maximum rotational speed parameter n_{max} and minimum rotational speed parameter n_{min}. As can be seen, all the obtained results of these parameters maintain a linear trend. However, it should be noted that the value of n_{max} increases significantly for scenarios 11-19 (power decrease) and little significantly for scenarios 1-9 (power increase). The reverse is true for the value of n_{min}, which decreases significantly for scenarios 1-9 (power increase) and insignificantly for scenarios 11-19 (power decrease).

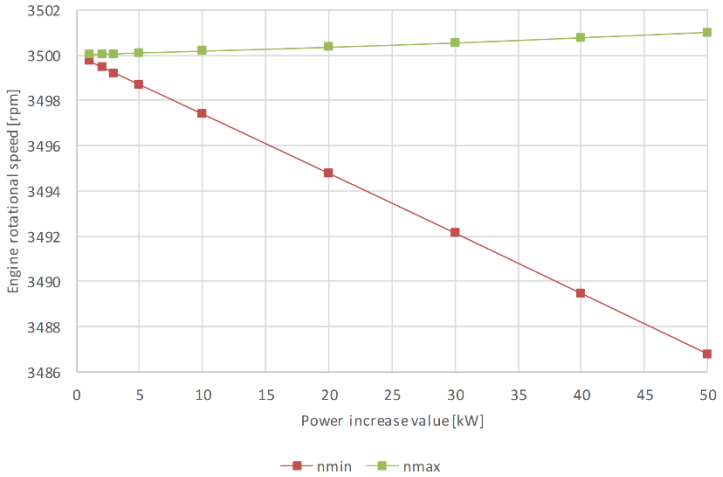

Fig. 10. Maximum rotational speed n_{max} and minimum rotational speed n_{min} for scenario 1-9 (power increase)

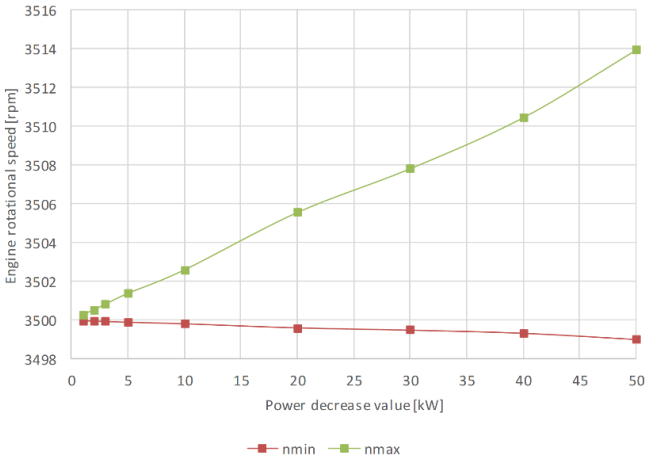

Fig. 11. Maximum rotational speed n_{max} and minimum rotational speed n_{min} for scenario 11-19 (power decrease)

Another parameter of time stabilization S_t represents the time required to stabilize the rotational speed value after changing the engine power. As a condition to confirm the stabilization of the engine rotational speed signal, the return to the nominal rotational speed value of 3500 rpm in five consecutive simulation time steps was set. As previously mentioned, the simulation time step is 0.0175 seconds. So the criteria of stabilization was made as no more than ±1 rpm changes from nominal rotational speed 3500 rpm in the total time of 0.0875 seconds. The stabilization time given in the figures below was calculated from the moment the engine power changed until the condition mentioned earlier was met. Its graphical interpretation can be seen in the figure above.

As can be seen in Fig. 12-13, in both cases of increasing or decreasing power, the S_t is characterized by a curve close to a logarithmic curve. However, for scenarios 1-9 compared to scenarios 11-19, it is significantly larger. For example, for a power change of 50 kW, it is 1.505 seconds compared to 1.295 seconds. This shows that the PI controller used stabilizes the rotational speed signal in a shorter time for decreasing power than for increasing motor power, which is the main conclusion of the presented research.

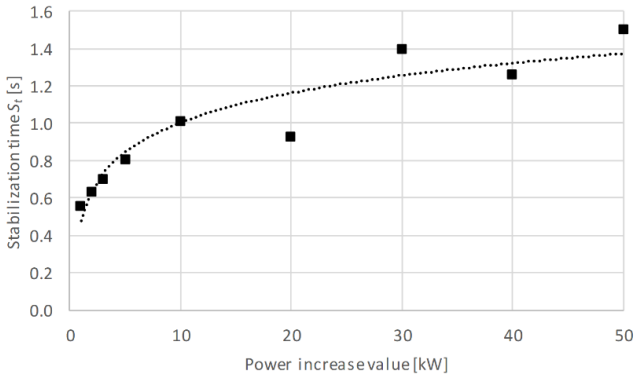

Fig. 12. Stabilization time S_t for scenario 1-9 (power increase)

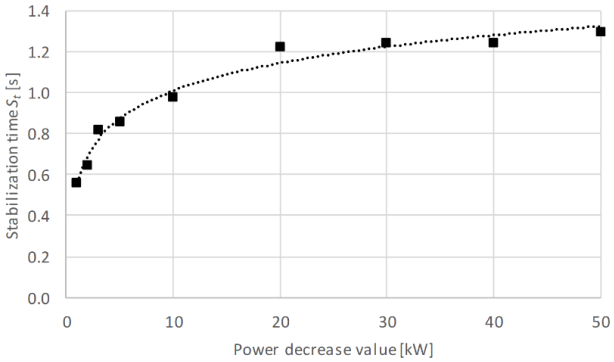

Fig. 13. Stabilization time S_t for scenario 11-19 (power decrease)

In order to compare the percentage difference of change shown in Fig. 12-13, scenario 1 was compared with scenario 11, scenario 2 with scenario 12, and so on, by relating them to the stabilization time comparison value parameter $S_{t\text{-}com}$ from the power increase scenarios, according to the equation below. The results are shown in Tab. 3.

$$S_{t-com} = \frac{S_{t1-9} - S_{t11-19}}{S_{t1-9}} \cdot 100\% \quad (3)$$

where: S_{t1-9} – stabilization time from scenario 1-9,
S_{t11-19} – stabilization time from scenario 11-19.

Tab. 3. Value of stabilization time comparison $S_{t\text{-}com}$

Scenario no.	1.	2.	3.	4.	5.	6.	7.	8.	9.
Stabilization time $S_{t\ scenario\ 1\text{-}9}$ [sec]	0.560	0.630	0.700	0.805	1.015	0.927	1.400	1.260	1.505
Scenario no.	11.	12.	13.	14.	15.	16.	17.	18.	19.
Stabilization time $S_{t\ scenario\ 11\text{-}19}$ [sec]	0.560	0.647	0.822	0.857	0.980	1.225	1.242	1.242	1.295
Stabilization time comparison $S_{t\text{-}com}$ [%]	-17.03	-9.11	-6.08	-3.21	-0.39	1.65	2.61	3.21	3.64

The value of St-com on the negative side indicates that the higher value of stabilization is for scenarios 11-19 (decreasing power), and the lower value is for scenarios 1-9 (increasing power). A positive value represents the opposite situation. From the data presented in the table, it can be seen that the PI controller used performs more favorably in power changes from 1 kW to 10 kW for increasing power, while in the higher range of power changes from 20 kW to 50 kW, better results are obtained for decreasing power.

4. CONCLUSIONS

The simulations and analyses conducted highlight the PI algorithm's effectiveness in improving light helicopter diesel engine performance. The research provides insights into potential challenges and limitations of such control systems, contributing to the development and optimization of helicopter propulsion technologies. The study offers tools and methods to enhance helicopter propulsion efficiency, reliability, and safety, with potential applications in other fields requiring precise diesel engine control.

Key findings include:

1. The use of a PI controller to control the rotational speed of a helicopter diesel engine requires different controller parameters depending on the change in the load torque on the rotor, i.e. different parameters when the torque is reduced and different when it is increased.
2. The PI controller for speed stabilization shows limited effectiveness when the torque changes are highly dynamic. Therefore, it is necessary to consider using different PI settings for different dynamic conditions or using a different type of controller.
3. The obtained values of the n_{dif} parameter are within acceptable limits for helicopter propulsion systems.
4. The values of the S_t parameter resulting from over-regulation are characterized by long times, exceeding 1 second, in the case of high dynamic torque changes.
5. Future research will focus on comparing the obtained control results of the PI algorithm to tests of other types of algorithms, including adaptive algorithms.
6. Conducting real-world tests to validate the results of simulation studies on a real object such as a helicopter equipped with a 330 kW Diesel engine is very demanding, so the authors plan to perform real-world tests on a smaller engine and under stationary conditions on an engine dynamometer.
7. Using the AVL Boost RT program allows simulating the behavior of an internal combustion engine under different control strategies. The use of a computer tool reduces the time required for such analysis. The same scope of work on a real object would be time-consuming and costly.

Acknowledgments

The research was financed within the framework of the Lublin University of Technology fund for conducting scientific activities FD - discipline fund, funded by the Polish Ministry of Science and Higher Education - Article 365 (2) of July 20, 2018.

REFERENCES

Ang, K. H., Chong, G., & Li, Y. (2005). PID control system analysis and design. *IEEE Transactions on Control Systems Technology*, *13*(4). 559-576. https://doi.org/10.1109/TCST.2005.847331

Åström, K. J., & Murray, R. M. (2008). *Feedback Systems: An Introduction for Scientists and Engineers*. Princeton University Press.

Banaszuk, A., Ariyur, K. B., Krstić, M., & Jacobson, C. A. (2004). An adaptive algorithm for control of combustion instability. *Automatica*, *40*(11), 1965-1972. https://doi.org/10.1016/j.automatica.2004.06.008

Beller, G., Árpád, I., Kiss, J. T., & Kocsis, D. (2021). AVL Boost: a powerful tool for research and education. *Journal of Physics Conference Series*, *1935*, 012015. https://doi.org/10.1088/1742-6596/1935/1/012015

Czyż, Z., Jakubczak, P., Podolak, P., Skiba, K., Karpiński, P., Droździel-Jurkiewicz, M., & Wendeker, M. (2023). Deformation measurement system for UAV components to improve their safe operation. *Eksploatacja i Niezawodność – Maintenance and Reliability*, *25*(4), 172358. https://doi.org/10.17531/ein/172358

Czyż, Z., Łusiak, T., Czyż , D., & Kasperek, D. (2016). Analysis of the pre-rotation engine loads in the autogyro. *Advances in Science and Technology. Research Journal*, *10*(31), 169-176. https://doi.org/10.12913/22998624/64015

Dudnika, V., & Gaponova, V. (2022). Correction system of the main rotor angular speed for helicopters of little weight categories. *Transportation Research Procedia*, 63, 187-194. https://doi.org/10.1016/j.trpro.2022.06.004

Heywood, J. B. (1988). *Internal Combustion Engine Fundamentals*. McGraw-Hill.

Hlinka, J., Kostial, R., & Horpatzka M. (2021). Application of enhanced methods for safety assessment of FADEC. *Maintenance and Reliability*, *23*(1), 63-73. https://doi.org/10.17531/ein.2021.1.7

Łusiak, T., & Grudzień, A. (2013). Rotor turbulence influence on helicopter flights in high urban built-up area. *Advances in Science and Technology Research Journal*, *7*(17), 47-50. https://doi.org/10.5604/20804075.1036997

Magryta, P. (2021). 1D modelling and PID control of helicopter diesel engine rotational speed in torque changes. *Journal of Physics: Conference Series*, *2130*, 012007. https://10.1088/1742-6596/2130/1/012007

Magryta, P., & Majczak, A. (2012). Diesel engine applicability in a light helicopter. *Autobusy: technika, eksploatacja, systemy transportowe*, 13(4), 98-103.

Mueller, T. J. (2002). *Introduction to the design of fixed-wing micro air vehicles: Including three case studies*. AIAA Education Series.

Niederliński, A., Mościński, J., & Ogonowski, Z. (1995). *Regulacja adaptacyjna.* Wydawnictwo Naukowe PWN.

Omran, I., Mostafa, A., Seddik, A., Ali, M., Hussein, M., Ahmed, Y., Aly, Y., & Abdelwahab, M. (2024). Deep reinforcement learning implementation on IC engine idle speed control. *Ain Shams Engineering Journal*, *15*(5): 102670. https://doi.org/10.1016/j.asej.2024.102670

Pietrykowski, K., Magryta, P., Wendeker, M., & Czyż, Z. (2014). Simulation studies of the helicopter diesel engine exploitation. *Logistyka*, *2014*(3), 5111-5117.

Przystupa, K. (2018). Tuning of PID controllers - Approximate methods. *Advances in Science and Technology Research Journal*, *12*(4), 56-64. https://doi.org/10.12913/22998624/99987

Stone, R. (1992). *Introduction to Internal Combustion Engines*. Palgrave Macmillan.

Wang, Y., Pan, M., Zhou, W., & Huang, J. (2023a). Direct thrust control for variable cycle engine based on fractional order PID-nonlinear model predictive control under off-nominal operation conditions. *Aerospace Science and Technology*, *143*, 108726. https://doi.org/10.1016/j.ast.2023.108726

Wang, Z., Du, J., & Guo, H. (2023b) A study on optimal rotor speed control method for helicopter power system considering the influence of infrared suppressors. *International Journal of Turbo & Jet-Engines*, *41*(3), 519-528. https://doi.org/10.1515/tjj-2023-0048

Wendeker, M., Siadkowska, K., Magryta, P., Czyż, Z., & Skiba, K. (2014). Optimal diesel engine technology analysis matching the platform of the helicopter. *World Academy of Science, Engineering and Technology International Journal of Mechanical, Industrial Science and Engineering*, *8*(5). https://doi.org/10.5281/zenodo.1092291

Zang, H., Changkai, Y., & Guoqiang, C. (2013). Variable rotor speed control for an integrated helicopter/engine system. *Proceedings of the Institution of Mechanical Engineers Part G Journal of Aerospace Engineering*, *228*(3), 323-341. https://doi.org/10.1177/0954410013485010